ESKİŞEHİR TECHNICAL UNIVERSITY JOURNAL OF SCIENCE AND TECHNOLOGY
A- APPLIED SCIENCES AND ENGINEERING

2020, 21(1), pp. 155 - 164, DOI: 10.18038/estubtda.675907

TEMPERATURE DEPENDENT (83-483 K) RAMAN SPECTROSCOPY ANALYSIS OF CVD GROWN WS_2 MONOLAYERS

Merve ÖPER[1], Nihan KOSKU PERKGÖZ[1,*]

[1] Electrical Electronics Department, Engineering Faculty, Eskişehir Technical University, Eskişehir, Turkey

ABSTRACT

For novel materials to be used in practical applications, their temperature dependent behavior and limitations need to be understood thoroughly. For example, the mobility of charge carriers, one of the important performance parameters in transistors, strongly depend on the change in the ambient temperature. Hence, characterization of potential optoelectronic materials at extreme temperatures is critical for future applications. In this study, we report on the changes of Raman scattering spectra as the temperature is changed from 83 K to 483 K for the 2D transition metal dichalcogenide materials, namely WS_2 monolayers formed by chemical vapor deposition technique (CVD). Our results show that both E′ (E^1_{2g}) and A_1(A_{1g}) modes red shift linearly as the temperature increases. The first order thermal coefficients have been calculated with the Grüneisen model, which suggests that in-plane mode is affected more by the increased temperature than that of out of plane mode. This difference is attributed to the defects in the sample as the flakes are grown by the CVD method. We also investigated the temperature dependence of the second order, 2LA(M) (at 345.7 cm^{-1}) which is one of the most intense peaks in the spectra.

Keywords: WS_2, Raman Spectroscopy, Temperature Dependence, Two-dimensional Materials

1. INTRODUCTION

Graphene is an exceptional, 2D material and their sheets offers high mobility (200 000 $cm^2\ v^{-1}\ s^{-1}$), high thermal conductivity (5300 W/mK) and high Young modulus (~1 TPa) [1-3] . It is a semimetal; it does not have an electronic bandgap around Fermi level, which means its valence and conduction bands touch each other at the Dirac point [4]. This is one of the most important obstacles for the graphene to commercialize in electronic applications, which results in a very low current on-off/ratio and excess heat dissipation when used in different active devices [5, 6]. Such drawbacks of graphene urged scientists to search for other two-dimensional materials, and transition metal dichalcogenide studies have been among the 2D materials that have drawn attention for future optoelectronic applications.

The common form of transition metal dichalcogenides (TMDs) is MX_2. M corresponds to an element from transition metal group -IV, V or VI- (Ti, Zr, V, Ta, Mo, W) and X is a chalcogen atom such as S, Se or Te; M is sandwiched between two chalcogen atoms [7]. We can categorize them as hexagonal, tetragonal or their distorted form, which depends on the arrangements of the atoms [8]. Generally, while interlayer bonds of TMDs are weak van der Waals type, their intralayer bonds are strong and covalent [9]. While these covalent bonds provide strong in-plane stability, the van der Waals bonds keep the stack together [10]. However, thanks to such weak van der Waals bonds, it is possible to obtain monolayer TMDs by using different techniques where even mechanical exfoliation can be used to isolate them [11]. Earlier theoretical and experimental studies unveiled that when we decrease the number of layers of TMDs, they exhibit a transition from indirect to direct band gap [12, 13]. For example, MoS_2 has an indirect bandgap of 1.29 eV in its bulk form, but when we reduce it to a monolayer, it becomes a direct bandgap material with a 1.90 eV bandgap [12]. WS_2 crystals also show a similar behavior, their bandgap is 1.3 eV in their bulk form, and become direct bandgap material, which is ~2.05 eV. For these TMDs, both the conduction bands (CB) and valence bands (VB) are located at the K points in the Brillouin zone

*Corresponding Author: nkperkgoz@eskisehir.edu.tr
Received: 05.03.2019 Published: 31.03.2020

which explains the formation of the direct bandgap in its monolayer form [14] . Monolayers TMDs show high photoluminescence and high absorbance so that they can be used in different optoelectrical applications such as solar cells, photodetectors, LEDs and lasers. However, large area production of TMD materials still hinders their wide usage in practical applications. In spite of its simplicity, mechanical exfoliation is not appropriate for large area production and an alternative method is required for large area-coverage of such monolayers with high quality. In our study, we have used chemical vapor deposition (CVD), to obtain uniform, high-quality, large-area flakes and films with rather low defect density in the structure [15, 16]. CVD is also the most widely used technique for large area growth of graphene.

2D WS_2 has rather low electron mass among the other TMDs, so it is expected to have relatively high electron mobility [17]. In earlier studies, monolayer WS_2 showed a mobility of 40-60 cm^2/Vs at room temperature, and since it is affected by impurities, surface roughness, defects, etc. mobility can be improved depending on the growth and preparation conditions [18-21].

Electron-phonon interactions have a critical impact on the performance of both optical and electronic properties. Therefore, understanding the vibrational characteristics of TMDs is essential for future applications [22]. In the earlier studies, researchers have investigated room temperature vibrational properties of the WS_2 flakes [23, 24]. Also, prior temperature-dependent studies of TMDs present that their growth techniques and their substrates affect the thermal characteristics of the structures [25-28]. In this study, we report an experimental investigation of Raman spectra of WS_2 single layers grown on Si/SiO_2 substrates where the temperature is changed from 83 K to 483 K to reveal their potential for the applications that are durable under harsh conditions such as space, defense, and marine.

2. EXPERIMENTAL PROCEDURE

In this study, we grow two-dimensional monolayer WS_2 flakes with chemical vapor deposition method and we use a special design two temperature zone CVD system. Before the experiments, we clean the Si/SiO_2 substrates with three solvent process (acetone, isopropanol and distilled water). We utilize WO_3 (Sigma-Aldrich, 99.5%) and sulfur (Sigma-Aldrich, 99.5%) as precursors and use N_2 gas as a carrier. Also, we make use of H_2 for its promoting effect [29]. We change the position of the furnace at 820°C and introduce WO_3 to react with sulfur. We wait for 3 minutes for the chemical reactions to form monolayer flakes. When the experimental procedure is over, we leave the furnace to cool down to the ambient temperature.

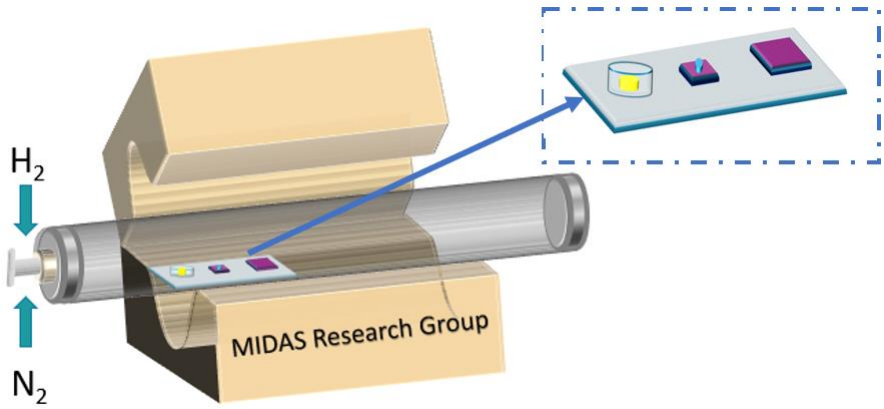

Figure 1. Two-zone (temperature) CVD system, inset shows the growth configuration including the precursors and substrate.

Raman spectroscopy analysis is the backbone of this study. In Figure 2, the working principle of our system is summarized. The difference between the wavelength of the laser and the scattered light will reveal the information on the crystal structure, lattice vibrations, flake thickness of TMDs and will serve

a fingerprint of the materials [30]. To perform temperature dependent measurements, we integrated a temperature stage (THMS600) to our Witec α-300 R μ-Raman system. Using this stage, we could cool down to low temperatures by liquid nitrogen and after performing the measurements, we increased the temperature step by step.

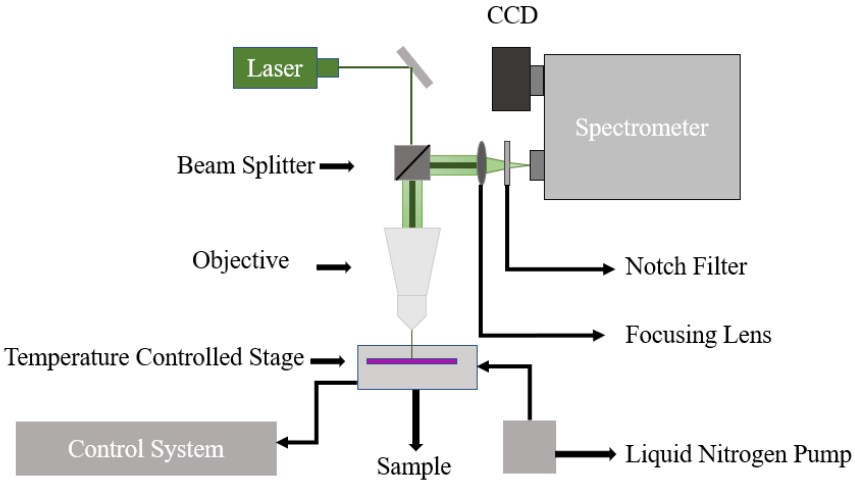

Figure 2. Working principle of μ-Raman Spectroscopy with the temperature control system

For the measurements, we used 50x (Numerical aperture=0.55) long distance objective with 9.1 mm free working distance. This working distance creates an opportunity for us to work with the temperature stage. Also, to obtain higher resolution, we used a higher grating option. It provides us higher grooves per mm, and this improves the scattering characteristic. Higher number of grooves causes higher scattering, and this increases the resolution of the measurements, so we chose 1200 groves/mm grating as the measurement parameter. For this measurement setup, our spatial resolution is 967.28 nm. We used a 532 nm laser source with 0.5 mW. We kept the power rather low not to increase the local temperature and avoid damaging the sample during the measurements. For this study, we have performed all measurements in the range of 83 K-483 K with 50 K steps.

In the literature, the Raman spectra of the monolayer WS_2 have already been reported showing that calculating the difference between the first-order modes at the Brillouin zone center (E′ and A_1) is a powerful tool to identify the number of layers of 2D WS_2. If the difference between E′- A_1 is lower than 64.5, the flakes are accepted as monolayers [29, 31]. For this reason, in the study, we mainly focus on E′ and A_1 modes (Figure 3b-d). Other modes in Figure 3a represent the longitudinal acoustic (LA) phonons at M point and additional peaks are multi-phonon combination of these modes [32, 33].

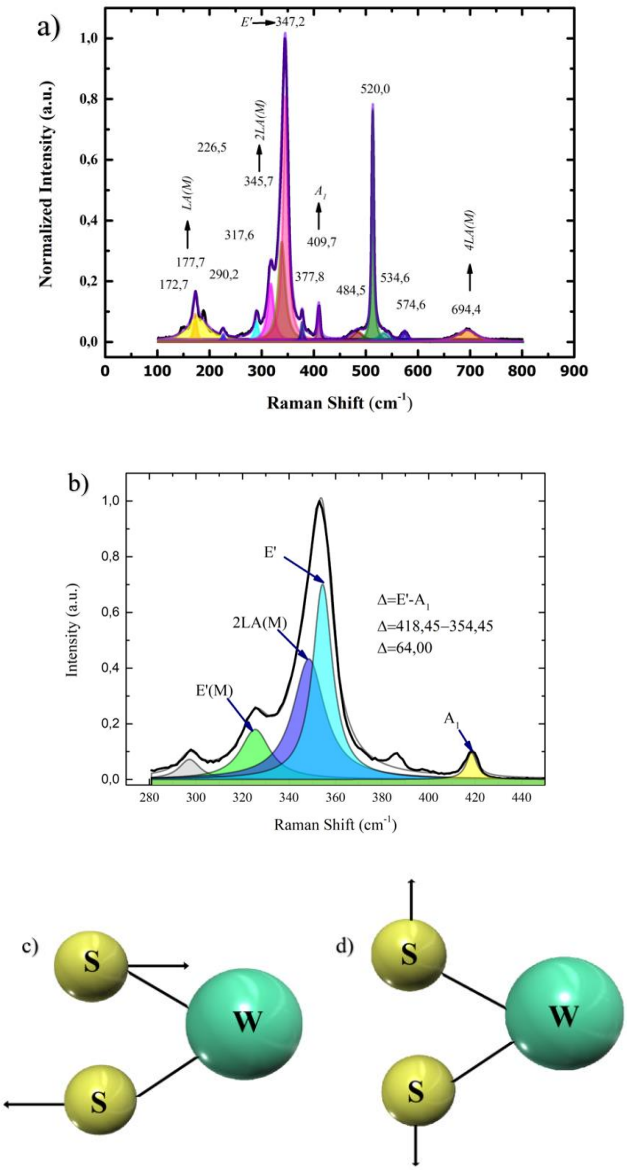

Figure 3. (a) Lorentzian fitted Raman spectrum of monolayer WS_2 (b) the peaks at the Brillouin zone; (c, d) schematic representation of a typical WS_2 structure with the sulfur atoms in yellow and the tungsten atoms in green for in-plane mode (E′) and out of plane mode (A_1), respectively.

3. RESULTS and DISCUSSIONS

Figure 4 presents the optical images of the CVD grown WS_2 monolayers where these images are taken at different temperatures; Figure 4a, 4b, 4c and 4d show the same sample at different temperatures such as 83 K, 283 K, 483 K and 608 K, respectively. WS_2 monolayers have not been damaged up to 608 K. This shows that WS_2 monolayer based devices will be durable even at extreme conditions such as very high temperatures. The Raman spectral measurements performed at 608 K are not included in the other graphs as the intensity of the measured signal at this temperature becomes very low.

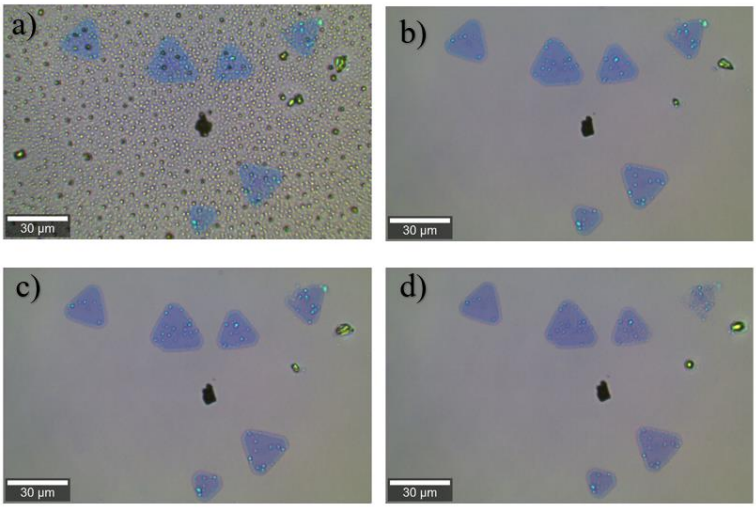

Figure 4. Optical image of the WS_2 flakes on Si/SiO_2 substrate with 50x magnification (a) at 83 K, (b) 283 K, (c) 483 K, (d) 608 K

Determining the peak parameters such as peak position, width, intensity, etc. is the goal of Raman peak fitting operation. Since we have sharp peaks in center without long wings, we choose to analyze our experimental data with Lorentzian Function [34]. After analyzing the data, we have separated E′ and A_1 modes, and we examined them separately. Grüneisen model provides a quantitative connection between thermal and mechanical properties [35]. We use it to obtain the first-order thermal coefficients of the sample. In Figure 5, we illustrate change the peak position of the E' and A_1 modes depending on the rising temperature. Then we fit our graph with Equation 1. In the equation, χ corresponds to the thermal coefficient and, ω_0 is the frequency of vibrations.

$$\omega(t)=\omega_0+\chi T \qquad (1)$$

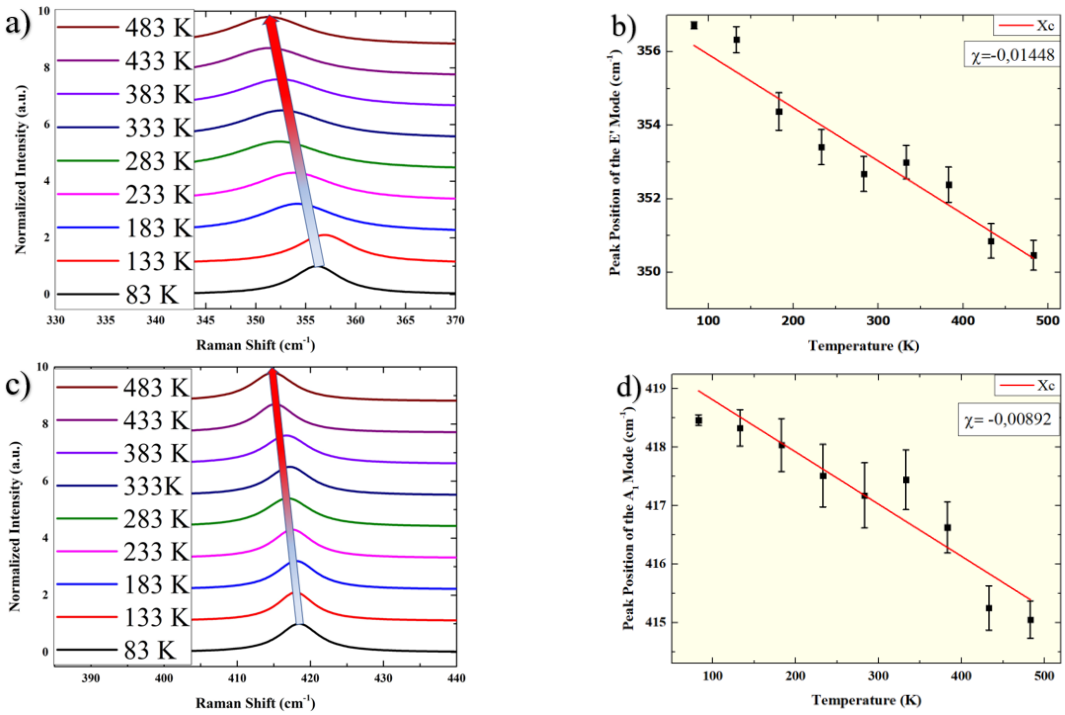

Figure 5. Raman shift of E' and A_1 modes as a function of temperature, respectively (a, c). Peak positions of E' and A_1 modes as a function of temperature, respectively (b, d).

The extracted thermal coefficient values for E' and A_1 modes are -0.01448 cm^{-1}/K and -0.00892 cm^{-1}/K, respectively. It can be seen from the data in Table 1 that the total redshifts of the centers from the starting point (83 K) to the finishing point (483 K) are 6.87 (from 357.30 cm^{-1} to 350.43 cm^{-1}) and 3.28 (from 418.54 cm^{-1} to 415.26 cm^{-1}) for E′ mode and A_1 mode, respectively. Our results show that temperature change affects E′ mode more than that of the A_1 mode. This can be explained by the combined effect of anharmonicity and thermal expansion of the flakes considering that E′ mode is in-plane. Also, the observed difference in the behavior of the modes can be attributed to the defects in the sample as the defects such as S deficiency, which becomes more significant with the increased temperature.

Table 1. Thermal coefficients and frequency shifts of the peak centers and FWHM values

		Thermal Coefficient (cm^{-1}/K)	**Peak Center Δw (cm^{-1})**	**FWHM Δw (cm^{-1})**
Modes	E'	-0.01448	6.87	6.42
	A_1	-0.00892	3.28	1.62

Also, the full width at half maximum (FWHM) of the peaks broadens with the escalating temperature. Anharmonicity changes the crystallinity of the material and increase in the temperature activates non-radiative recombination mechanisms. As a consequence, they cause the peaks to broaden with a shift of the peak centers (Figure 6) [36, 37]. As the thermal energy becomes higher, the scattering rate is enhanced. In addition to this, with the increasing anharmonicity, the overtone peaks such as the ones at 228.2 and 377.6 cm^{-1} become more visible in the Raman spectra when they are deconvoluted.

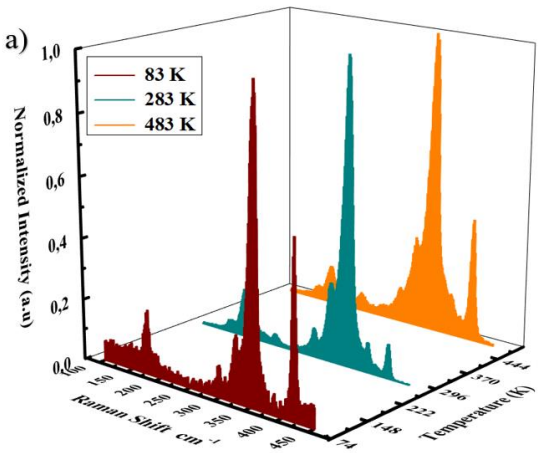

Figure 6. Three-dimensional representation of normalized intensity vs Raman shift at 83, 283 and 483 K.

2LA(M) (at 345.7 cm^{-1}) is a second order mode but at room temperature, it approximately has twice the intensity of A_1 mode [33]. To examine this relationship regarding the temperature effect on these modes, we draw the curve representing the ratio: (intensity of 2LA(M)) / (intensity of A_1) in Figure 7. At very low and very high temperatures, we observe an unexpected behavior with a significant decrease of the ratio for both low and high temperature cases. We attribute this change to the scattering mechanisms. At low temperatures, impurities affect the scattering and with the increased temperature, probability of lattice scattering enhances [38]. Such higher level of lattice scattering can be caused by anharmonicity. We suggest abnormal impurity scattering at low temperatures due to inefficient purging process. Icing on the sample can cause the decreasing of the intensity (Figure 4 (a)). Since 2LA(M) is a second order mode, it can be affected from the occurrence of the additional scattering processes.

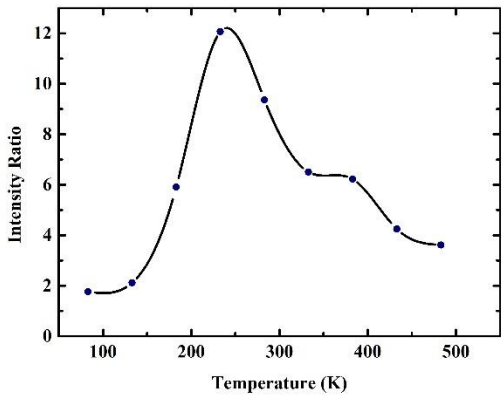

Figure 7. The intensity ratio of 2LA(M) and A_1 modes, (intensity of 2LA(M)) / (intensity of A_1)

4. CONCLUSIONS

In conclusion, we have systematically examined the Raman shifts of different modes of the CVD grown WS_2 flakes on Si/SiO_2 samples within the range of 83 K and 483 K. First of all, we have demonstrated that our atomically thin layers which were grown by CVD are durable down to very low (83 K) and up to very high (608 K) temperatures. With the increased temperature, both E′ and A_1 modes exhibit redshift and broadening in the modes, which can be explained primarily due to change in the anharmonicity and suggestively due to thermal expansion. In addition to this, the A_1 mode shows less temperature dependence. This can be related to the more dominant effect of defects on the in plane (E′) mode. Our experimental results provide information on the fundamental thermal parameters of the CVD grown monolayer WS_2 flakes, which is a critical step for the design of novel optoelectronic applications based on two-dimensional transition metal dichalcogenides at extreme temperatures.

ACKNOWLEDGEMENTS

This work was supported by Eskişehir Technical University Research Project Numbers: BAP 19ADP050, BAP 19ADP052 and TUBITAK Project No: 116F445.

REFERENCES

[1] Bolotin, K.I., K.J. Sikes, Z. Jiang, M. Klima, G. Fudenberg, J. Hone, P. Kim, and H. Stormer, *Ultrahigh electron mobility in suspended graphene.* Solid State Communications, 2008. 146(9-10): p. 351-355.

[2] Balandin, A.A., S. Ghosh, W. Bao, I. Calizo, D. Teweldebrhan, F. Miao, and C.N. Lau, *Superior thermal conductivity of single-layer graphene.* Nano letters, 2008. 8(3): p. 902-907.

[3] Bunch, J.S., A.M. Van Der Zande, S.S. Verbridge, I.W. Frank, D.M. Tanenbaum, J.M. Parpia, H.G. Craighead, and P.L. McEuen, *Electromechanical resonators from graphene sheets.* Science, 2007. 315(5811): p. 490-493.

[4] Reddy, D., L.F. Register, G.D. Carpenter, and S.K. Banerjee, *Graphene field-effect transistors.* Journal of Physics D: Applied Physics, 2011. 44(31): p. 313001.

[5] Palacios, T., A. Hsu, and H. Wang, *Applications of graphene devices in RF communications.* IEEE Communications Magazine, 2010. 48(6): p. 122-128.

[6] Bosi, M., *Growth and synthesis of mono and few-layers transition metal dichalcogenides by vapour techniques: a review.* RSC Advances, 2015. 5(92): p. 75500-75518.

[7] Wang, Q.H., K. Kalantar-Zadeh, A. Kis, J.N. Coleman, and M.S. Strano, *Electronics and optoelectronics of two-dimensional transition metal dichalcogenides.* Nature nanotechnology, 2012. 7(11): p. 699.

[8] Choi, W., N. Choudhary, G.H. Han, J. Park, D. Akinwande, and Y.H. Lee, *Recent development of two-dimensional transition metal dichalcogenides and their applications.* Materials Today, 2017. 20(3): p. 116-130.

[9] Voiry, D., A. Mohite, and M. Chhowalla, *Phase engineering of transition metal dichalcogenides.* Chemical Society Reviews, 2015. 44(9): p. 2702-2712.

[10] Geim, A.K. and I.V. Grigorieva, *Van der Waals heterostructures.* Nature, 2013. 499(7459): p. 419-425.

[11] Eda, G., H. Yamaguchi, D. Voiry, T. Fujita, M. Chen, and M. Chhowalla, *Photoluminescence from Chemically Exfoliated MoS2.* Nano Letters, 2011. 11(12): p. 5111-5116.

[12] Mak, K.F., C. Lee, J. Hone, J. Shan, and T.F. Heinz, *Atomically thin MoS 2: a new direct-gap semiconductor.* Physical review letters, 2010. 105(13): p. 136805.

[13] Amin, B., T.P. Kaloni, and U. Schwingenschlögl, *Strain engineering of WS 2, WSe 2, and WTe 2.* Rsc Advances, 2014. 4(65): p. 34561-34565.

[14] Zhang, Y., T.-R. Chang, B. Zhou, Y.-T. Cui, H. Yan, Z. Liu, F. Schmitt, J. Lee, R. Moore, and Y. Chen, *Direct observation of the transition from indirect to direct bandgap in atomically thin epitaxial MoSe 2.* Nature nanotechnology, 2014. 9(2): p. 111.

[15] Elías, A.L., N. Perea-López, A. Castro-Beltrán, A. Berkdemir, R. Lv, S. Feng, A.D. Long, T. Hayashi, Y.A. Kim, M. Endo, et al., *Controlled Synthesis and Transfer of Large-Area WS2 Sheets: From Single Layer to Few Layers.* ACS Nano, 2013. 7(6): p. 5235-5242.

[16] Lee, Y.-H., L. Yu, H. Wang, W. Fang, X. Ling, Y. Shi, C.-T. Lin, J.-K. Huang, M.-T. Chang, C.-S. Chang, et al., *Synthesis and Transfer of Single-Layer Transition Metal Disulfides on Diverse Surfaces.* Nano Letters, 2013. 13(4): p. 1852-1857.

[17] Ovchinnikov, D., A. Allain, Y.-S. Huang, D. Dumcenco, and A. Kis, *Electrical transport properties of single-layer WS2.* ACS nano, 2014. 8(8): p. 8174-8181.

[18] Jo, S., N. Ubrig, H. Berger, A.B. Kuzmenko, and A.F. Morpurgo, *Mono-and bilayer WS2 light-emitting transistors.* Nano letters, 2014. 14(4): p. 2019-2025.

[19] McCreary, K.M., A.T. Hanbicki, S. Singh, R.K. Kawakami, G.G. Jernigan, M. Ishigami, A. Ng, T.H. Brintlinger, R.M. Stroud, and B.T. Jonker, *The effect of preparation conditions on Raman and photoluminescence of monolayer WS 2.* Scientific reports, 2016. 6: p. 35154.

[20] Iqbal, M.W., M.Z. Iqbal, M.F. Khan, M.A. Shehzad, Y. Seo, J.H. Park, C. Hwang, and J. Eom, *High-mobility and air-stable single-layer WS 2 field-effect transistors sandwiched between chemical vapor deposition-grown hexagonal BN films.* Scientific reports, 2015. 5: p. 10699.

[21] Late, D.J., B. Liu, H.S.S.R. Matte, V.P. Dravid, and C.N.R. Rao, *Hysteresis in Single-Layer MoS2 Field Effect Transistors.* ACS Nano, 2012. 6(6): p. 5635-5641.

[22] Sahoo, S., A.P. Gaur, M. Ahmadi, M.J.-F. Guinel, and R.S. Katiyar, *Temperature-dependent Raman studies and thermal conductivity of few-layer MoS2.* The Journal of Physical Chemistry C, 2013. 117(17): p. 9042-9047.

[23] Şar, H., A. Özden, B. Yorulmaz, C. Sevik, N.K. Perkgoz, and F. Ay, *A comparative device performance assesment of CVD grown MoS 2 and WS 2 monolayers.* Journal of Materials Science: Materials in Electronics, 2018. 29(10): p. 8785-8792.

[24] Gutiérrez, H.R., N. Perea-López, A.L. Elías, A. Berkdemir, B. Wang, R. Lv, F. López-Urías, V.H. Crespi, H. Terrones, and M. Terrones, *Extraordinary room-temperature photoluminescence in triangular WS2 monolayers.* Nano letters, 2012. 13(8): p. 3447-3454.

[25] Thripuranthaka, M., R.V. Kashid, C. Sekhar Rout, and D.J. Late, *Temperature dependent Raman spectroscopy of chemically derived few layer MoS2 and WS2 nanosheets.* Applied Physics Letters, 2014. 104(8): p. 081911.

[26] Su, L., Y. Yu, L. Cao, and Y. Zhang, *Effects of substrate type and material-substrate bonding on high-temperature behavior of monolayer WS 2.* Nano Research, 2015. 8(8): p. 2686-2697.

[27] Late, D., *Temperature dependent phonon shifts in single-layer WS (2).* ACS applied materials & interfaces, 2014. 6(2): p. 1158-1163.

[28] Pawbake, A.S., M.S. Pawar, S.R. Jadkar, and D.J. Late, *Large area chemical vapor deposition of monolayer transition metal dichalcogenides and their temperature dependent Raman spectroscopy studies.* Nanoscale, 2016. 8(5): p. 3008-3018.

[29] Yorulmaz, B., A. Özden, H. Şar, F. Ay, C. Sevik, and N.K. Perkgöz, *CVD growth of monolayer WS2 through controlled seed formation and vapor density.* Materials Science in Semiconductor Processing, 2019. 93: p. 158-163.

[30] Zhang, X., Q.-H. Tan, J.-B. Wu, W. Shi, and P.-H. Tan, *Review on the Raman spectroscopy of different types of layered materials.* Nanoscale, 2016. 8(12): p. 6435-6450.

[31] Shi, W., M.-L. Lin, Q.-H. Tan, X.-F. Qiao, J. Zhang, and P.-H. Tan, *Raman and photoluminescence spectra of two-dimensional nanocrystallites of monolayer WS2 and WSe2.* 2D Materials, 2016. 3(2): p. 025016.

[32] Sourisseau, C., F. Cruege, M. Fouassier, and M. Alba, *Second-order Raman effects, inelastic neutron scattering and lattice dynamics in 2H-WS2.* Chemical physics, 1991. 150(2): p. 281-293.

[33] Berkdemir, A., H.R. Gutiérrez, A.R. Botello-Méndez, N. Perea-López, A.L. Elías, C.-I. Chia, B. Wang, V.H. Crespi, F. López-Urías, and J.-C. Charlier, *Identification of individual and few layers of WS 2 using Raman spectroscopy.* Scientific reports, 2013. 3: p. 1755.

[34] Bradley, M.S., *Lineshapes in IR and Raman spectroscopy: A primer.* Spectroscopy, 2015. 30(11): p. 42-+.

[35] Stacey, F.D. and J.H. Hodgkinson, *Thermodynamics with the Grüneisen parameter: Fundamentals and applications to high pressure physics and geophysics.* Physics of the Earth and Planetary Interiors, 2019. 286: p. 42-68.

[36] Gurioli, M., A. Vinattieri, M. Colocci, C. Deparis, J. Massies, G. Neu, A. Bosacchi, and S. Franchi, *Temperature dependence of the radiative and nonradiative recombination time in GaAs/Al x Ga 1− x As quantum-well structures.* Physical Review B, 1991. 44(7): p. 3115.

[37] Yang, M., X. Cheng, Y. Li, Y. Ren, M. Liu, and Z. Qi, *Anharmonicity of monolayer MoS2, MoSe2, and WSe2: A Raman study under high pressure and elevated temperature.* Applied Physics Letters, 2017. 110(9): p. 093108.

[38] Streetman, B.G. and S. Banerjee, *Solid State Electronic Devices*. 2001: Prentice-Hall of India.